Molecular Cell
Short Article

# Live Cell Imaging of Telomerase RNA Dynamics Reveals Cell Cycle-Dependent Clustering of Telomerase at Elongating Telomeres

Franck Gallardo,[1,3,4] Nancy Laterreur,[2,3] Emilio Cusanelli,[1] Faissal Ouenzar,[1] Emmanuelle Querido,[1] Raymund J. Wellinger,[2,*] and Pascal Chartrand[1,*]
[1]Département de Biochimie, Université de Montréal, Montréal, QC H3C 3J7, Canada
[2]Département de Microbiologie et Infectiologie, Université de Sherbrooke, Sherbrooke, QC J1H 5N4, Canada
[3]These authors contributed equally to this work
[4]Present address: Laboratoire de Biologie Moléculaire Eucaryote, Université Paul Sabatier, Centre National de la Recherche Scientifique, Unité Mixte de Recherche 5099, 31062 Toulouse, France
*Correspondence: p.chartrand@umontreal.ca (P.C.), raymund.wellinger@usherbrooke.ca (R.J.W.)
DOI 10.1016/j.molcel.2011.09.020

## SUMMARY

**The telomerase, which is composed of both protein and RNA, maintains genome stability by replenishing telomeric repeats at the ends of chromosomes. Here, we use live-cell imaging to follow yeast telomerase RNA dynamics and recruitment to telomeres in single cells. Tracking of single telomerase particles revealed a diffusive behavior and transient association with telomeres in G1 and G2 phases of the cell cycle. Interestingly, concurrent with telomere elongation in late S phase, a subset of telomerase enzyme clusters and stably associates with few telomeres. Our data show that this clustering represents elongating telomerase and it depends on regulators of telomerase at telomeres (MRX, Tel1, Rif1/2, and Cdc13). Furthermore, the assay revealed premature telomere elongation in G1 in a *rif1/2* strains, suggesting that Rif1/2 act as cell-cycle dependent negative regulators of telomerase. We propose that telomere elongation is organized around a local and transient accumulation of several telomerases on a few telomeres.**

## INTRODUCTION

Telomeres are essential nucleoprotein structures that form the ends of eukaryotic chromosomes. Due to intrinsic problems of replicating DNA ends, telomeric DNA shortens during each cell division (Hug and Lingner, 2006; O'Sullivan and Karlseder, 2010). This attrition is counteracted by the action of an end-specialized and relatively well-conserved enzyme called telomerase (Greider and Blackburn, 1987), which was reviewed by Shore and Bianchi (2009). The telomerase holoenzyme is composed of both protein and RNA, and its functions rely on proper trafficking and assembly of these components (Hug and Lingner, 2006). The *Saccharomyces cerevisiæ* telomerase is composed minimally of an RNA molecule (*TLC1* RNA), which contains the template sequence and the protein catalytic reverse-transcriptase, Est2 (Counter et al., 1997; Lingner et al., 1997; Singer and Gottschling, 1994). Other factors, such as the regulatory subunits Est1 and Est3, also are required for telomerase activity at telomeres (Evans and Lundblad, 1999; Lundblad and Szostak, 1989), and the yKu70/80 complex is thought to be important for telomerase retention at telomeres (Gallardo et al., 2008; Peterson et al., 2001; Shore and Bianchi, 2009).

Current studies on telomerase regulation at telomeres depend heavily on chromatin immunoprecipitation (ChIP), which provides snapshots of telomerase association with telomeres in a large population of cells. For budding yeast cells, ChIP studies have hypothesized that Est2, the telomerase catalytic subunit, and *TLC1*, the telomeric RNA, are both associated with telomeres from G1 to late S phase (Fisher et al., 2004; Taggart et al., 2002). These results also lead to a telomerase-activation model, in which telomerase is present on telomeres in G1 and S phase, but in an inactive form. In late S phase, only the shortest telomeres would be elongated via a local activation of telomerase (Hug and Lingner, 2006; Shore and Bianchi, 2009; Taggart et al., 2002). Alternatively, a recruitment model posits that an interaction between Cdc13, the single-strand telomeric binding protein, and Est1 preferentially recruits the telomerase holoenzyme to short telomere ends, leading to their elongation (Evans and Lundblad, 1999; Shore and Bianchi, 2009). This latter model is supported by genetic data, which revealed that the Cdc13-Est1 interaction is essential for telomere elongation and that a Cdc13-Est2 fusion protein can bypass the essential function of Est1 (Evans and Lundblad, 1999; Pennock et al., 2001). Moreover, both Cdc13 and Est1 are preferentially enriched at telomeres in late S phase cells, as shown by ChIP (Taggart et al., 2002).

Because current techniques are inadequate to unambiguously distinguish between these models, new approaches must be developed to study the cell-cycle regulation of telomerase and its recruitment to telomeres. Recent advances in live-cell imaging technologies allow a determination of the dynamics of a specific molecule, either protein or nucleic acid, in single living cells. These techniques thus provide unique and potentially conclusive approaches to study the association and dynamics of a specific factor with chromatin (Voss and Hager, 2008).

Thus, they should allow an assessment of the dynamics of telomerase localization and association with telomeres in single living cells in a way that has not been explored yet.

Given that telomerase holoenzyme assembly and trafficking are intimately associated with its function (Gallardo et al., 2008; Venteicher et al., 2009), we began to investigate the cell-cycle dependent regulation of telomerase at a molecular level in living cells. For this purpose, we developed a green fluorescent protein (GFP) reporter system to visualize the yeast telomerase RNA. Because *TLC1* RNA limits telomerase assembly and activity in budding yeast (Mozdy and Cech, 2006), it is the ideal marker for studying the dynamics of telomerase holoenzyme. Real time acquisition of particle movements shows that during G1 and G2 phases of the cell cycle, telomerase particles behave in a diffusive manner and do not stably interact with telomeres. However, concurrent with telomere elongation in late S phase, a subset of telomerase RNA molecules clusters and associates with a small number of telomeres. This clustering depends on factors that regulate telomerase recruitment at telomeres (e.g., MRX, Tel1, Rif1, Rif2, and Cdc13), and the data strongly suggests that these striking foci represent actively elongating telomerase. The experiments also reveal that Rif1 and Rif2 act as cell-cycle dependent negative regulators of telomere elongation because they restrict telomerase access to telomeres outside of S-phase. Taken together, these results for the first time reconcile disparate sets of molecular models for the cell-cycle dependent regulation of telomerase at telomeres. In contrast to previous suggestions, our data show that telomerase is not stably associated with telomeres during most of the cell cycle. Such an association is prevented, at least in part, by the Rif-proteins and, surprisingly, in their absence, telomeres can be elongated even during G1 of the cell cycle. However, during late S-phase telomere elongation is organized around a local and transient accumulation of several telomerases on a few telomeres.

## RESULTS

### Development of an Assay to Visualize *TLC1* RNA in Living Yeast Cells

We used a GFP reporter system to visualize the trafficking of *TLC1* RNA in living cells. The system is based on MS2 RNA stem-loops incorporated into the *TLC1* RNA and the MS2 coat protein fused to a fluorescent GFP moiety (Bertrand et al., 1998; Querido and Chartrand, 2008). The *TLC1* RNA used here was expressed on a plasmid and contains ten MS2 stem-loops inserted just upstream of the mature 3′-end (*TLC1-10* × *MS2*, Figures 1A and S1 available online). The second component comprises an MS2 RNA-binding protein fused to GFP (MS2-GFP) that lacks a nuclear localization sequence and, thus, diffuses between the nucleus and the cytoplasm. *Tlc1Δ* yeasts expressing both *TLC1-10* × *MS2* RNA and MS2-GFP displayed wild-type telomere length and no apparent growth arrest phenotype normally associated with a lack of *TLC1* RNA (Figure S1). Further, immunoprecipitation of MS2 complexes followed by telomeric primer extension assay confirmed that the *TLC1-10* × *MS2* RNA was incorporated into active telomerase complexes (Figure S1). Finally, as determined by fluorescence in situ hybridization using *TLC1* RNA-specific probes in combination with GFP imaging, coexpression of *TLC1-10* × *MS2* RNA and MS2-GFP resulted in the formation of several small nuclear foci in which the GFP signal and the *TLC1-10* × *MS2* RNA colocalized (Figure 1B). Thus, the *TLC1-10* × *MS2* RNA/MS2-GFP complex (hereafter called *TLC1* RNA-GFP) fully complements a *tlc1* deletion and the position of GFP-foci represents the localization of the telomerase RNA in living cells.

### Live Cell Imaging of Green Fluorescent Protein-Labeled *TLC1* RNA

To explore the dynamics of *TLC1* RNA with respect to the cell-cycle stage, sequential imaging of living yeast cells maintained under normal growth conditions was performed. Surface plot analysis of foci fluorescence intensities showed that, in G1 and G2, the *TLC1* RNA-GFP foci have a rather homogenous fluorescence distribution (Figure 1C, Movie S1), suggesting comparable numbers of RNA molecules per focus. Moreover, tracking of the foci revealed that the *TLC1-10* × *MS2* RNA displayed a diffusive behavior in G1 cells, with velocities averaging 499 nm/s (Figure 2A). Mean square displacement (MSD) analysis confirmed a diffusive behavior for *TLC1* RNA-GFP particles (Figure 2B), with either free or corralled displacement, as previously described for free mRNA (Shav-Tal et al., 2004). However, these particles did not correspond to protein-free *TLC1-10* × *MS2* RNA molecules because immunoprecipitated *TLC1* RNA-GFP particles from G1-arrested cells demonstrated a telomerase activity, suggesting that these RNA are associated with Est2 (Figure S2). In G2 cells, *TLC1* RNA-GFP foci displayed the same dynamics and homogeneity as in G1 (Figure 1C and Movie S2).

To compare the dynamics of the *TLC1* RNA-GFP with its substrate (i.e., the telomeres), we used a yeast strain containing a 256 × LacO array integrated near telomere $IV_R$ (Heun et al., 2001). After imaging and tracking LacI-GFP particles in the same conditions as *TLC1* RNA-GFP foci, we assessed the dynamics of telomere $IV_R$ (Figure S2 and Movie S4). During G1 and G2, movement of telomere $IV_R$ was much slower than *TLC1* RNA-GFP foci, with a nearly 2-fold difference in both velocity and displacement and a 5-fold difference in the diffusion coefficient (Figure 2A). These telomere $IV_R$ data are consistent with previous measurements of the dynamics of telomeres in yeast, which also showed that their dynamics do not change during the cell cycle (Bystricky et al., 2005). Moreover, MSD analysis of telomere particles during G1 and G2 of the cell cycle revealed a much more static behavior of telomeres compared to *TLC1* RNA-GFP foci (Figure 2B), showing that the *TLC1* RNA is more dynamic than telomeres in these phases of the cell cycle.

### *TLC1* RNA Clustering in Late S Phase

Previously, ChIP experiments had been used to study the association of telomerase proteins and telomerase recruitment factors with telomeres during the various phases of the cell cycle (Fisher et al., 2004; Taggart et al., 2002). The results suggested an increase of the interactions of telomerase components with telomeres during late S phase, the time when telomere elongation occurs (Fisher et al., 2004; Hug and Lingner, 2006; Marcand et al., 2000; Taggart et al., 2002). It was, therefore, of particular interest to assess *TLC1* RNA-GFP dynamics in late S phase cells. Interestingly, some *TLC1* RNA-GFP foci were observed

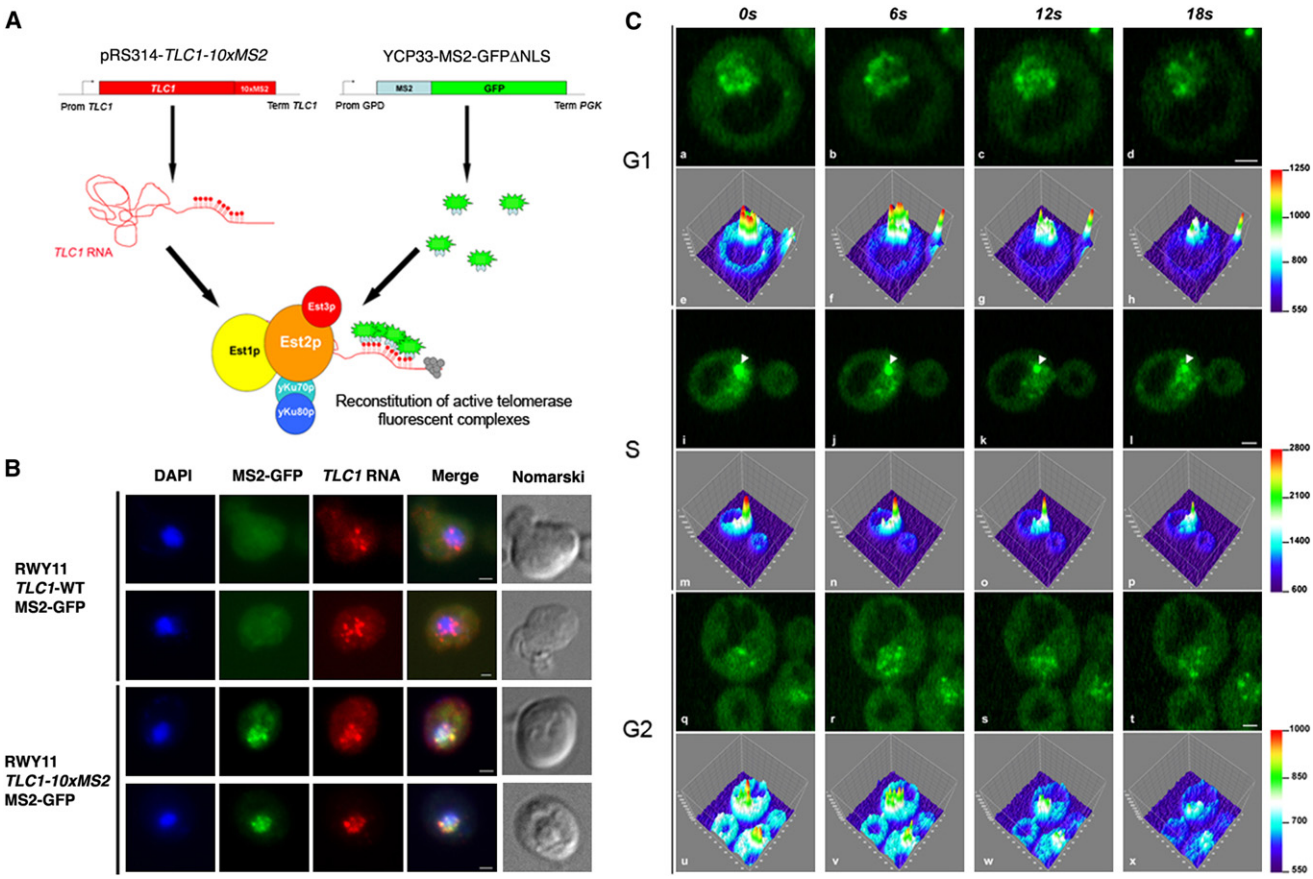


**Figure 1. A Green Fluorescent Reporter System to Visualize Telomerase RNA in Living Yeast Cells**

(A) Description of the MS2-GFP reporter system.

(B) Fluorescent in situ hybridization on *TLC1* RNA shows colocalization between *TLC1-10xMS2* RNA and MS2-GFP foci. Scale bar: 1 μm.

(C) Time-lapse images (taken from Movies S1, S2, and S3 at the indicated times) of cells in G1 (a–d); S phase (i–l); and G2 (q–t) expressing *TLC1* RNA-GFP foci. Frames extracted from movies were converted in fluorescence intensity profiles of *TLC1* RNA-GFP in G1 (e–h); S phase (m–p); and G2 (u–x) cells. White arrowhead indicates *TLC1* RNA-GFP cluster. Color code (right side) reflects arbitrary fluorescence intensity. Scale bar: 1 μm.

that were at least three times bigger and two times brighter than those observed during G1 or G2 (Figures 1C and S1). Quantification of the fluorescence revealed a 6- to 15-fold enrichment in *TLC1* RNA-GFP, suggesting the clustering of several *TLC1-10* × *MS2* RNA molecules. However, not all *TLC1-10* × *MS2* RNA accumulated in these clusters, as smaller foci were still visible in these very same cells, albeit fewer than in G1 or G2 cells. These intense clusters were observed almost exclusively in late S phase cells (Figure 2C), with 40% of cells containing one cluster and fewer cells containing two or three clusters (Figure 2D). Time-lapse imaging of an early S phase cell over a period of 40 min revealed that a small *TLC1* RNA-GFP cluster appeared after 20 min (mid-S phase), increased in fluorescence, and remained until the end of S phase (Figure S2). Using fast imaging and particle tracking, the dynamic parameters of these clusters were also determined (Movies S3 and S4). Interestingly, all three parameters of the S phase clusters (i.e., velocity, displacement, and diffusion coefficient), were similar to those of telomere $IV_R$ (Figure 2A), and MSD behavior of the clusters was indistinguishable from those of telomere $IV_R$ (Figure 2B). The fact that telomerase RNA clusters into intense foci only in late S phase, but not in the G1 or G2 phases of the cell cycle, and that these clusters have the same dynamics as telomeres, strongly suggests that S phase clustering of *TLC1* RNA-GFP represents a temporary association of telomerase with telomeres. Therefore, we propose to call these clusters telomerase recruitment clusters (T-Recs).

## The Formation of Telomerase Recruitment Clusters Is Linked to Telomere Elongation

To directly determine whether T-Recs represent telomere-associated *TLC1* RNA in late S phase cells, colocalization between telomerase RNA and telomeres was assessed using multicolor imaging in live cells. Telomeres were visualized using a Rap1-mCherry fusion protein, a telomere-associated protein that has been used to detect telomeres in living yeast (Schober et al., 2008). Indeed, during G1, *TLC1* RNA-GFP foci displayed a very transient (<5 s) colocalization with Rap1-mCherry-tagged telomeres (Figure 3A and Movie S5). In sharp contrast, in late S phase cells, *TLC1* RNA-GFP clusters displayed a stable

A

| | # of particles | # of frames | Particle Velocity (nm/s) | | | Displacement (nm) | | | D ($\mu m^2/s$)[a] |
|---|---|---|---|---|---|---|---|---|---|
| | | | Min | Max | Avg | Min | Max | Avg | |
| *TLC1-GFP (G1)* | 15 | 367 | 335 | 729 | 499 | 67 | 177 | 118 | 0,0601 |
| *TLC1-GFP (S)* | 11 | 890 | 196 | 309 | 227 | 37 | 61 | 48 | 0,0069 |
| *TLC1-GFP (G2/M)* | 14 | 331 | 246 | 745 | 550 | 49 | 191 | 115 | 0,0523 |
| *TEL IV$_R$-LacO$_{256}$* | 10 | 1298 | 198 | 433 | 293 | 39 | 86 | 59 | 0,0098 |

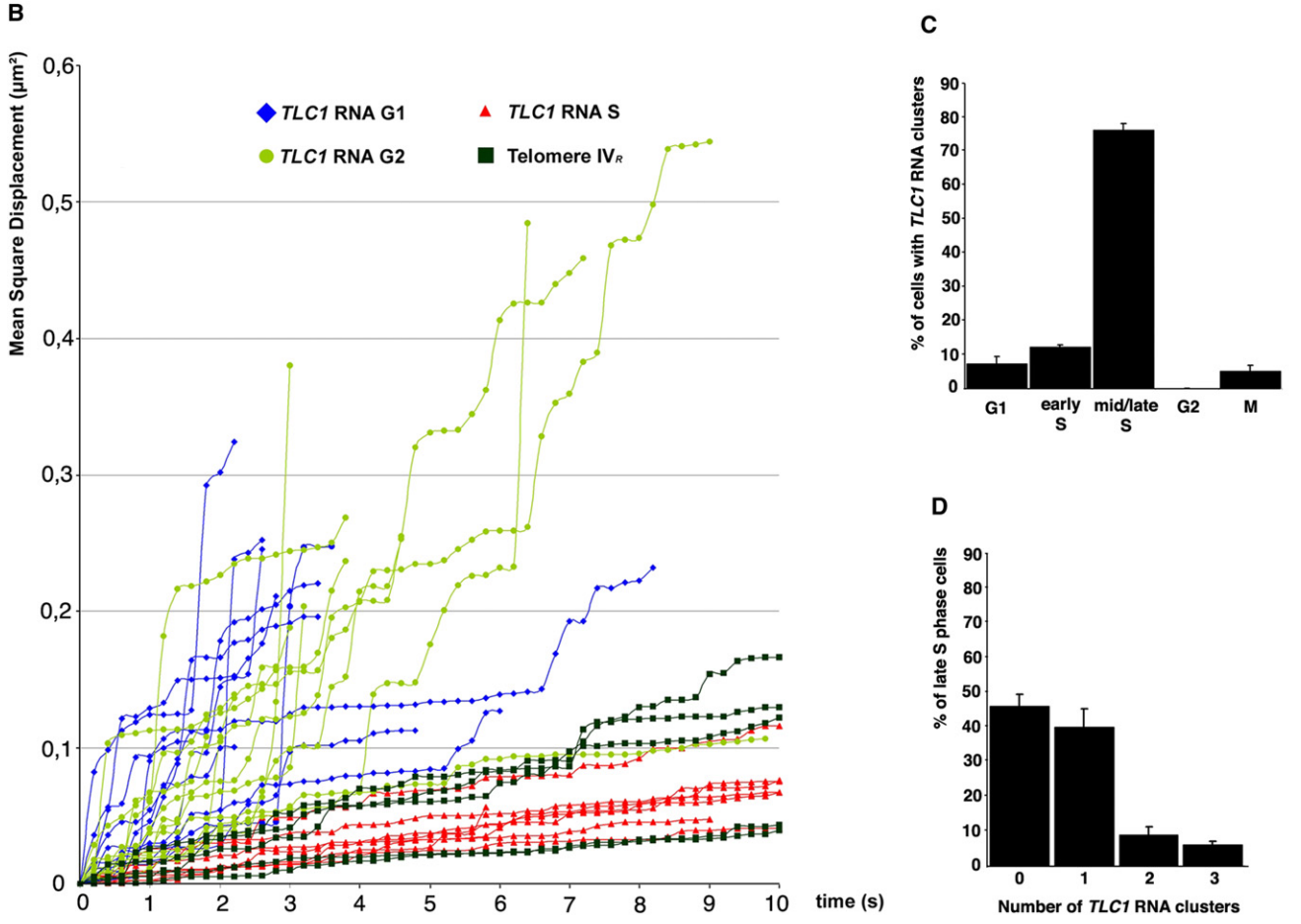


**Figure 2. Dynamics of *TLC1* RNA-GFP Foci and Clusters**

(A) Comparison of *TLC1* RNA-GFP particle dynamics in different phases of the cell cycle; a diffusion coefficient (D).

(B) Comparison of the MSD of *TLC1* RNA-GFP foci in G1 or G2, *TLC1* RNA-GFP clusters in S phase, and *TEL IV$_R$*-LacO foci.

(C) Occurrence of *TLC1* RNA-GFP clusters during cell-cycle phases.

(D) Quantification of the number of *TLC1* RNA-GFP cluster per late S phase cell.

colocalization with only one telomere cluster (Figure 3A and Movie S5). Quantification of colocalization between *TLC1* RNA-GFP and Rap1-mCherry-tagged telomeres revealed that *TLC1* RNA-GFP foci in G1 displayed a maximal residence time of 5 s on a telomeric cluster, whereas T-Recs in late S phase had residence times up to 45 s (Figure 3B). Thus, these results demonstrate that the T-Recs observed in late S phase are indeed telomere-associated *TLC1* RNAs. However, only a subset of telomeres appears to be involved in any single observable event.

If the formation of T-Recs was functionally linked to telomere elongation, their appearance should be affected by mutations in genes involved in telomerase recruitment/activation and also by those inhibiting telomerase-mediated telomere lengthening. Therefore, T-Recs occurrence was measured in strains lacking *XRS2* or *TEL1*, two factors that promote telomerase recruitment to short telomeres (Arnerić and Lingner, 2007; Goudsouzian et al., 2006; Shore and Bianchi, 2009). In late S phase, 55% of wild-type cells displayed at least one T-Rec, but this percentage dropped to less than 15% in *xrs2Δ* and *tel1Δ* strains (Figure 3C). Furthermore, T-Rec occurrence was also measured in a *cdc13-2* mutant strain. This allele of *CDC13* specifically disrupts the interaction between the single-strand G-tail binding protein Cdc13 and Est1, an interaction that is essential for telomere elongation by telomerase (Pennock et al., 2001). In cells harboring this

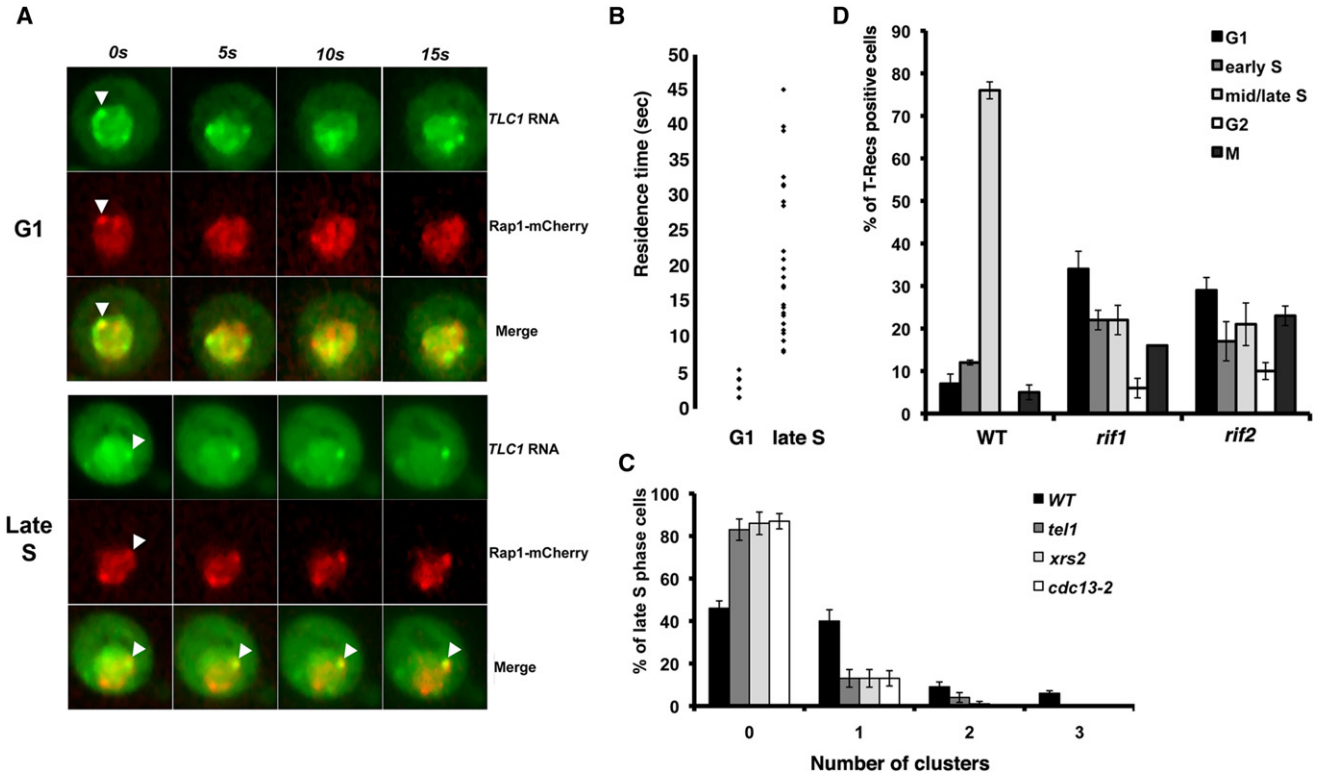


**Figure 3. T-Recs Are Associated with Telomere**

(A) Stable colocalization between *TLC1* RNA-GFP and the telomeric marker Rap1-mCherry occurs in S phase cells. White arrowheads indicate colocalizing *TLC1* RNA-GFP and Rap1-mCherry (telomeres) in G1 (top) or an S phase cell (bottom). Panels show 5 s time points of dual-color movies.

(B) Residence time of *TLC1* RNA on a telomeric cluster, either as *TLC1* RNA-GFP foci in G1 (n = 19) or T-Recs in late S phase cells (n = 25).

(C) Deletion of positive regulators of telomerase recruitment to telomeres reduces T-Recs occurrence.

(D) Deletion of negative regulators of telomerase abolishes cell cycle-regulated occurrence of T-Recs.

*cdc13-2* allele, a single T-Rec was observed in only 13% of late S phase cells and cells with multiple T-Recs could no longer be detected, strongly suggesting that T-Recs represent functional telomerase molecules clustered on a telomere. To be consistent with the above results, T-Rec occurrence should increase in cells harboring mutations in negative regulators of telomerase activity, such as *RIF1* and *RIF2* (Wotton and Shore, 1997). Indeed, we observed a 3-fold increase in T-Rec-positive cells in *rif2* versus wild-type cells (31 ± 4% versus 10 ± 2% of total cells, respectively). Remarkably, in mutants lacking either *RIF1* or *RIF2*, the hitherto S phase-restricted occurrence of T-Recs was completely lost and T-Recs became detectable in all phases of the cell cycle (Figure 3D). In this particular setting, the occurrence of T-Recs during G1 in *rif1* and *rif2* mutant cells predicts that telomere elongation can occur in this phase of the cell cycle. To explore this possibility, we used an assay based on the induction of a single short telomere by the Flp1 recombinase (Marcand et al., 1999). The elongation of the induced single short telomere by telomerase during G1 or after release from G1 was measured in both wild-type and *rif2* mutant strains. For both strains, cell synchronization in G1 with α-factor, FLP-mediated telomere shortening, and subsequent release into the cell cycle led to elongation of the single shortened telomere (Figures 4A and S3). As expected from previous data, G1-arrested wild-type cells showed no measurable elongation of the shortened telomere (Figures 4A and S3). Interestingly, and as predicted by the T-Recs analysis discussed previously, telomere elongation was observed in *rif2* cells even while they were maintained in G1 (Figure 4A). Preliminary results obtained with the identical experimental setup, but using *rif1* cells, yielded comparable telomere elongation in G1-arrested cells as in released cells (data not shown). These data strongly suggest that the Rif1/2 proteins control the cell-cycle dependent access of telomerase to telomeres. Altogether, our results show that T-Recs represent actively elongating telomerase visualized in living cells.

Our hypothesis also predicted that the number of T-Recs should correlate with the number of potentially elongating, short telomeres. To test this idea, *yku70-30*, a temperature-sensitive mutant of *YKU70*, was used. In cells harboring this allele and incubated at 37°C, telomeres are as short as they are in Yku-lacking cells, but upon temperature downshift to 23°C, telomeres elongate in a telomerase-dependent fashion (Gravel and Wellinger, 2002). Y*ku70* null strains expressing *TLC1*-GFP and either a plasmid-borne wild-type or temperature-sensitive *yku70-30* allele were grown at 23°C and then shifted to 37°C for 12 hr. Thereafter, the temperature was shifted back to 23°C for 2 hr, and T-Recs positive S-phase cells were assessed for the distribution of the number of observed T-Recs. As expected,

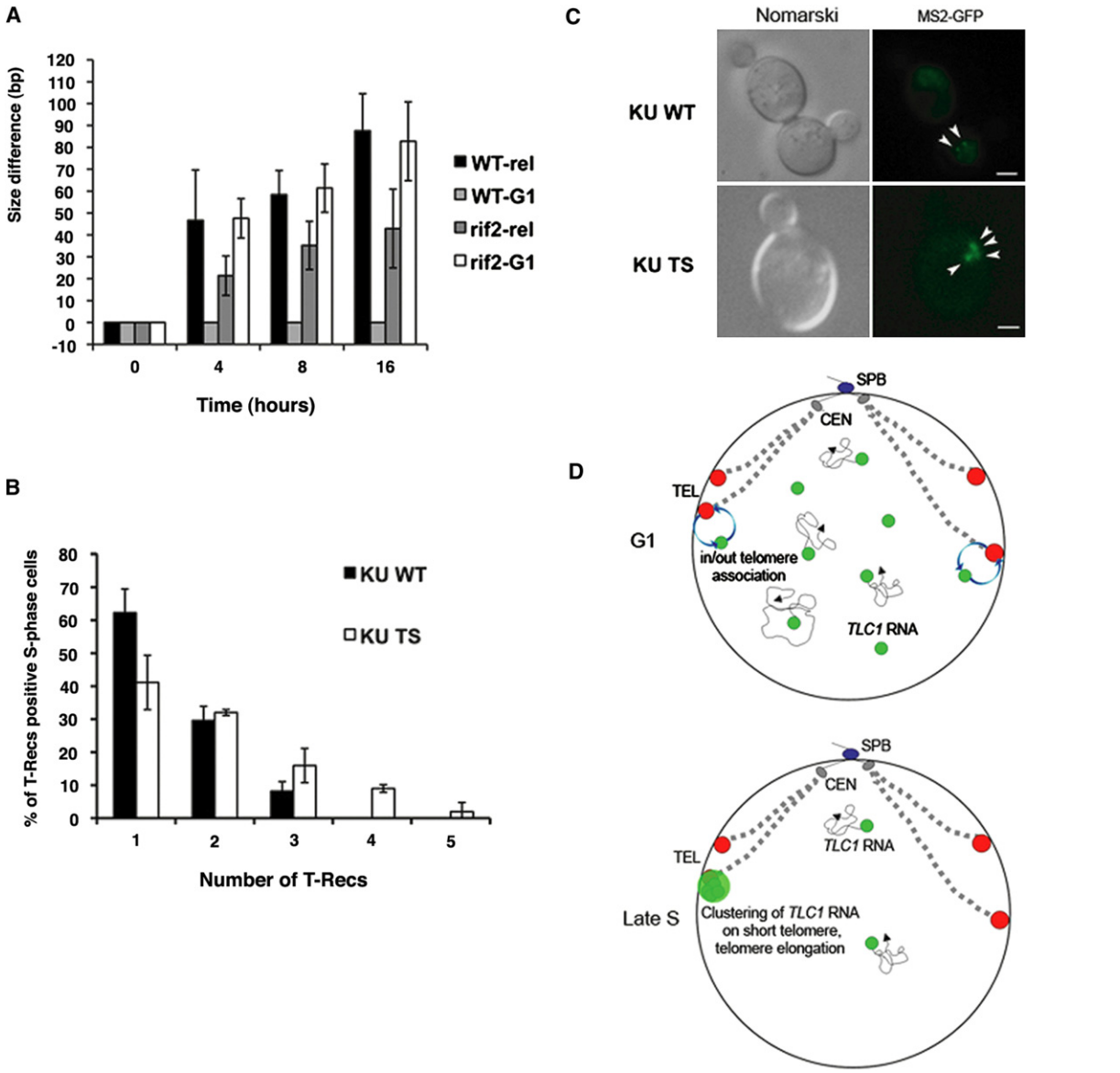


**Figure 4. T-Recs Are Linked to Telomere Elongation**

(A) Rif2 represses telomere elongation in G1. Elongation (in base pairs) of a single short telomere in a wild-type (WT) or *rif2* yeast strain. Cells were synchronized in G1 with α-factor prior to inducing the shortening of a single telomere. Cells were either released from G1 (WT-rel and *rif2*-rel) or maintained in G1 (WT-G1 and *rif2*-G1) for the indicated periods.

(B) Quantification of the number of T-Recs per late S phase cell in cells with normal (KU WT) or shorter (KU TS) telomeres.

(C) Examples of late S phase cells with two T-Recs (KU WT) or four T-Recs (KU TS). Scale bar: 1 μm.

(D) Model of telomerase RNA dynamics in a G1 or late S phase cell. SPB, spindle pole body; CEN: centromere; TEL; telomere.

over 60% of cells in wt cells with *YKU70* displayed one T-Rec and there was a maximum of three T-Recs per T-Rec-positive cell. However, in *yku70-30* cells recovering from high temperature incubation and in which virtually all telomeres required lengthening, the distribution of T-Recs occurrence clearly shifted to higher numbers. Indeed, we observed cells with four or even five T-Recs, a situation never found in wt cells (see above; Figures 4B and 4C). We conclude that T-Rec occurrence reflects clustered *TLC1* RNA molecules during active telomere elongation.

## DISCUSSION

Our results document for the first time the visualization and tracking of telomerase RNA particles in real time in single living cells. Our data support a model in which telomere elongation depends on the stable recruitment of several telomerase molecules to a few telomeres only in late S phase (Figure 4D). Indeed, our results show that *TLC1* RNA is not stably associated with telomeres in G1 and G2 but, rather, diffuses inside the nucleus with dynamic parameters only consistent with free or corralled

diffusion. Previous ChIP and fluorescence in situ hybridization (FISH) experiments revealed an interaction between telomerase RNA and Est2 with telomeres in G1 and early S phase (Fisher et al., 2004; Gallardo et al., 2008; Taggart et al., 2002), suggesting the presence of a *TLC1* RNA-Est2 complex at telomeres before telomere elongation. Our results now suggest that this interaction is transient, albeit detectable by ChIP, and that a stable association of *TLC1* RNA with telomeres occurs only in late S phase, in the form of the *TLC1* RNA clusters reported here. We call T-Recs the S phase-specific, stable association of *TLC1* RNA with telomeres in the form of *TLC1* RNA clusters.

How these clusters assemble is not yet clear. Because evidence suggests that yeast telomerase may act as a dimer or multidimer in vivo, T-Recs may correspond to an oligomerization of telomerase during telomere elongation (Prescott and Blackburn, 1997). Nevertheless, our data do show that T-Recs are linked to telomere elongation, because mutants affecting telomerase recruitment and elongation of telomeres (*tel1*, *xrs2*, and *cdc13-2*) disrupt *TLC1* RNA clustering. Moreover, a transient shortening of all telomeres, using a temperature-sensitive mutant of *YKU70* and followed by reactivation of YKu activity, resulted in increased numbers of T-Recs per cell, which supports the link between *TLC1* RNA clustering and telomere elongation. Finally, our results are in agreement with the estimated number of telomeres elongated per cell cycle. Indeed, the frequency of telomere elongation in telomerase-positive cells containing normal telomere lengths is around 6%–8%, meaning that fewer than 3 telomeres should be elongated at each round of division (Teixeira et al., 2004). The number of T-Recs per cell that we measured (between 1 and 3) is consistent with this observation.

Our data also revealed a novel role for Rif1 and Rif2 in cell-cycle dependent regulation of telomerase-mediated telomere replication. Deletion of either *RIF1* or *RIF2* resulted in the accumulation of T-Recs in all the phases of the cell cycle, suggesting that the overextended telomere phenotype observed in these mutants may be due to telomere elongation outside of S phase. Indeed, in G1-arrested *rif1 or rif2* cells, but not in arrested wild-type cells, a single abruptly shortened telomere can be extended, further supporting this hypothesis. Taken together, our results suggest that Rif-proteins inhibit access to telomeres by telomerase throughout the cell cycle, except in late S phase, after the passage of the replication fork (Dionne and Wellinger, 1998; Wellinger et al., 1996). This hypothesis is consistent with the fact that in cells lacking Rif-proteins, the frequency of individual telomere elongation events increases in telomerase-positive cells with normal telomere lengths, whereas the actual amount of added repeats per elongation event remains about the same as in wild-type (Teixeira et al., 2004).

## EXPERIMENTAL PROCEDURES

### Live Cell Imaging

Multicolor live cell imaging and acquisition for particle tracking was realized using a Leica DMI6000B motorized spinning disk confocal microscope with a 100× Leica PL APO 1.4NA lens (1pixel = 0,099nm). Confocal imaging was realized with a diode laser for GFP (491 nm/25 mW) with GFP fluorescence filters (520/35). A temperature control chamber and objective heater was used to maintain temperature at 30°C. Digital images were acquired with a Hamamatsu 9100 EM-CCD camera with binning at 1 (512*512BT). Image acquisition was done using Volocity software with exposure set at 200 ms for tracking and 400 ms for multicolor imaging with 80%–100% laser power and autocontrast ON. Under these imaging conditions, phototoxicity was reduced, as cells still have the ability to grow normally after imaging (data not shown). Cell cycle phase was assessed by morphologic criteria and bud- mother index (BMI) to discriminate between late S phase and G2 (BMI between 0,3 and 0,7).

### Particle Tracking and Surface Plot Analysis

Stacks were imported using Image J software (http://rsbweb.nih.gov/ij/) corrected for photobleaching, and particles were tracked using the particle detector and tracker module plugin using the following parameters. For small *TLC1* RNA-GFP foci: radius = 2; cutoff = 0; percentile between 0,1 and 0,5; link = 2; displacement = 8. For *TLC1* RNA-GFP clusters: radius = 3; cutoff = 0; percentile = 0,1; link = 2; displacement = 8. All tracks generated by the plugin were visually inspected to fit particle position in every frame. Only tracks superior to 13 time points were included in the analysis. Examples of tracks generated for telomere $IV_R$ and *TLC1* RNA-GFP are shown in Movie S4. Because Image J output provides only particle position (in X,Y) at each time point, velocity and mean square displacement were extracted by mathematical conversion in Excel software. Velocity vectors were calculated with the formula $\|\vec{V}\| = \sqrt{(x_i - x_{i-1})^2 + (y_i - y_{i-1})^2}$. After integrating calibration and exposition times, velocities are displayed in nm/s (min, max and average) (Figure 2A).

For MSD calculation, X-Y coordinates for each time points were used in the formula

$$MSD = \sum_{0-i} \left[ \sqrt{(x_i - x_0)^2 + (y_i - y_0)^2} - \sqrt{(x_{i-1} - x_0)^2 + (y_{i-1} - y_0)^2} \right]^2.$$

After integrating calibration and exposition times, MSD are displayed in $\mu m^2$. Calculation of the diffusion coefficient was realized by measuring the average initial slope of the MSD curves. The difference in diffusion coefficient (D) between the *TLC1* RNA-GFP foci in G1 cells and the clusters in late S phase cells cannot be explained by simple aggregation and, therefore, reduced mobility of telomerase complexes. According to the Stokes-Einstein law of diffusion, the diffusion coefficient of a molecule is proportional to the cube of its mass ($D \propto M^3$) (Bacia et al., 2006). Therefore, a 9-fold decrease in D observed between *TLC1* RNA-GFP foci (in G1 phase) versus clusters (in S phase) would require the aggregation of a number of *TLC1* RNA molecules exceeding the estimated total pool of molecules available by orders of magnitude.

### Quantitative Analysis of TLC1 RNA-GFP Foci and Telomerase Recruitment Clusters

We define a *TLC1* RNA-GFP focus as a small (304 ± 49 nm), highly mobile fluorescent dot observed in the nucleus of G1, S and G2 cells. The *TLC1* RNA-GFP clusters, or T-Recs, are 2- to 3-fold larger than foci (684 ± 134 nm). They are immobile or much less mobile than the foci and present mostly in mid/late S phase.

For scoring of *TLC1* RNA-GFP clusters, cells grown at 30°C to $OD_{600}$ between 0.2 and 0.3 were counted directly under a Nikon E800 epifluorescence microscope equipped with a 100× Nikon DIC H (1.4NA) lens. A minimum of 50 cells were scored in three independent experiments. For cell-cycle distribution of T-Recs, only T-Rec-positive cells were scored. For the number of T-Recs per late S phase cell, cells in late S phase were randomly scored, and the number of cells with 0, 1, or more T-Recs was counted using epifluorescence microscopy. We used epifluorescence microscopy to score the T-Recs because these clusters, but not the small *TLC1* RNA-GFP foci, are clearly visible with this microscope.

For quantification of the residence time of *TLC1* RNA-GFP foci and T-Recs on Rap1-mCherry-labeled telomeres, two-color acquisition movies were analyzed and the colocalization time of foci or T-Recs on Rap1-mCherry foci was quantified. For T-Recs, the movies analyzed lasted 8–68 s, or an average acquisition time of 27 s. For *TLC1* RNA-GFP foci, movies lasted 21–72 s, or an average acquisition time of 47 s.

### Telomere Elongation Assay

The experiments were performed as described in (Marcand et al., 1999), with slight modifications. Briefly, LEV336 *bar1::TRP1* and LEV336 *bar1::TRP1 rif2::KAN* cells were grown to an $OD_{600}$ of 0.3 in rich media containing 2% raffinose and then G1-arrested using 0.1 or 1 μM α-factor (Bioshop) for 90 min. The Flp1 recombinase was induced for 90 min by the addition of galactose, 2% final. Thereafter, cells were collected by centrifugation, thoroughly rinsed, resuspended, and then either allowed to enter cycling or kept arrested in G1 by readdition of α-factor (1 μM) in rich media containing 2% glucose. Samples were taken at indicated time points. After 8 h, α-factor was again added to arrested cultures. Cell-cycle arrest was monitored by cell morphology using a light microscope and FACS analysis.

Genomic DNA, which was isolated from cells at the indicated time points, was extracted using a standard glass beads method. After digestion with StuI, samples were migrated on a 0.6% agarose gel. Southern blotting was performed and the membrane was hybridized with either *ADH4* (Marcand et al., 1999) or a *pCT300* probe, a 300-bp fragment containing 280 bp of telomeric repeats derived from pYLPV (Wellinger et al., 1993). Telomeric fragment sizes were determined using ImageQuant by measuring the distance between the induced TRF and the residual FRT product.

## SUPPLEMENTAL INFORMATION

Supplemental Information includes three figures, five movies, Supplemental Experimental Procedures, and Supplemental References and can be found with this article online at doi:10.1016/j.molcel.2011.09.020.

## ACKNOWLEDGMENTS

We thank S. Marcand and D. D'Amours for yeast strains and plasmids, P. Maddox for technical advice, C. Glowinsky for technical help using Imaris, and A. Kamgoue for MSD and diffusion coefficient calculation. We also thank the Cell Imaging and Analysis Network (CIAN) at McGill University for access to its imaging resources. This work was supported by Canadian Institutes of Health Research grants MOP97874 to R.J.W. and MOP89768 to P.C. F.G. was supported by a doctoral fellowship from the Terry Fox Foundation. P.C. is a Senior Scholar from the Fonds de la Recherche en Santé du Québec and R.J.W. holds a Canada Research Chair.

Received: March 31, 2011
Revised: June 21, 2011
Accepted: September 12, 2011
Published: December 8, 2011

## REFERENCES

Arnerić, M., and Lingner, J. (2007). Tel1 kinase and subtelomere-bound Tbf1 mediate preferential elongation of short telomeres by telomerase in yeast. EMBO Rep. *8*, 1080–1085.

Bacia, K., Kim, S.A., and Schwille, P. (2006). Fluorescence cross-correlation spectroscopy in living cells. Nat. Methods *3*, 83–89.

Bertrand, E., Chartrand, P., Schaefer, M., Shenoy, S.M., Singer, R.H., and Long, R.M. (1998). Localization of ASH1 mRNA particles in living yeast. Mol. Cell *2*, 437–445.

Bystricky, K., Laroche, T., van Houwe, G., Blaszczyk, M., and Gasser, S.M. (2005). Chromosome looping in yeast: telomere pairing and coordinated movement reflect anchoring efficiency and territorial organization. J. Cell Biol. *168*, 375–387.

Counter, C.M., Meyerson, M., Eaton, E.N., and Weinberg, R.A. (1997). The catalytic subunit of yeast telomerase. Proc. Natl. Acad. Sci. USA *94*, 9202–9207.

Dionne, I., and Wellinger, R.J. (1998). Processing of telomeric DNA ends requires the passage of a replication fork. Nucleic Acids Res. *26*, 5365–5371.

Evans, S.K., and Lundblad, V. (1999). Est1 and Cdc13 as comediators of telomerase access. Science *286*, 117–120.

Fisher, T.S., Taggart, A.K.P., and Zakian, V.A. (2004). Cell cycle-dependent regulation of yeast telomerase by Ku. Nat. Struct. Mol. Biol. *11*, 1198–1205.

Gallardo, F., Olivier, C., Dandjinou, A.T., Wellinger, R.J., and Chartrand, P. (2008). TLC1 RNA nucleo-cytoplasmic trafficking links telomerase biogenesis to its recruitment to telomeres. EMBO J. *27*, 748–757.

Goudsouzian, L.K., Tuzon, C.T., and Zakian, V.A. (2006). S. cerevisiae Tel1p and Mre11p are required for normal levels of Est1p and Est2p telomere association. Mol. Cell *24*, 603–610.

Gravel, S., and Wellinger, R.J. (2002). Maintenance of double-stranded telomeric repeats as the critical determinant for cell viability in yeast cells lacking Ku. Mol. Cell. Biol. *22*, 2182–2193.

Greider, C.W., and Blackburn, E.H. (1987). The telomere terminal transferase of Tetrahymena is a ribonucleoprotein enzyme with two kinds of primer specificity. Cell *51*, 887–898.

Heun, P., Laroche, T., Shimada, K., Furrer, P., and Gasser, S.M. (2001). Chromosome dynamics in the yeast interphase nucleus. Science *294*, 2181–2186.

Hug, N., and Lingner, J. (2006). Telomere length homeostasis. Chromosoma *115*, 413–425.

Lingner, J., Hughes, T.R., Shevchenko, A., Mann, M., Lundblad, V., and Cech, T.R. (1997). Reverse transcriptase motifs in the catalytic subunit of telomerase. Science *276*, 561–567.

Lundblad, V., and Szostak, J.W. (1989). A mutant with a defect in telomere elongation leads to senescence in yeast. Cell *57*, 633–643.

Marcand, S., Brevet, V., and Gilson, E. (1999). Progressive cis-inhibition of telomerase upon telomere elongation. EMBO J. *18*, 3509–3519.

Marcand, S., Brevet, V., Mann, C., and Gilson, E. (2000). Cell cycle restriction of telomere elongation. Curr. Biol. *10*, 487–490.

Mozdy, A.D., and Cech, T.R. (2006). Low abundance of telomerase in yeast: implications for telomerase haploinsufficiency. RNA *12*, 1721–1737.

O'Sullivan, R.J., and Karlseder, J. (2010). Telomeres: protecting chromosomes against genome instability. Nat. Rev. Mol. Cell Biol. *11*, 171–181.

Pennock, E., Buckley, K., and Lundblad, V. (2001). Cdc13 delivers separate complexes to the telomere for end protection and replication. Cell *104*, 387–396.

Peterson, S.E., Stellwagen, A.E., Diede, S.J., Singer, M.S., Haimberger, Z.W., Johnson, C.O., Tzoneva, M., and Gottschling, D.E. (2001). The function of a stem-loop in telomerase RNA is linked to the DNA repair protein Ku. Nat. Genet. *27*, 64–67.

Prescott, J., and Blackburn, E.H. (1997). Functionally interacting telomerase RNAs in the yeast telomerase complex. Genes Dev. *11*, 2790–2800.

Querido, E., and Chartrand, P. (2008). Using Fluorescent Proteins to Study mRNA Trafficking in Living Cells. Methods Cell Biol. *85*, 273–292.

Schober, H., Kalck, V., Vega-Palas, M.-A., Van Houwe, G., Sage, D., Unser, M., Gartenberg, M.R., and Gasser, S.M. (2008). Controlled exchange of chromosomal arms reveals principles driving telomere interactions in yeast. Genome Res. *18*, 261–271.

Shav-Tal, Y., Darzacq, X., Shenoy, S.M., Fusco, D., Janicki, S.M., Spector, D.L., and Singer, R.H. (2004). Dynamics of single mRNPs in nuclei of living cells. Science *304*, 1797–1800.

Shore, D., and Bianchi, A. (2009). Telomere length regulation: coupling DNA end processing to feedback regulation of telomerase. EMBO J. *28*, 2309–2322.

Singer, M.S., and Gottschling, D.E. (1994). TLC1: template RNA component of Saccharomyces cerevisiae telomerase. Science *266*, 404–409.

Taggart, A.K.P., Teng, S.-C., and Zakian, V.A. (2002). Est1p as a cell cycle-regulated activator of telomere-bound telomerase. Science *297*, 1023–1026.

Teixeira, M.T., Arneric, M., Sperisen, P., and Lingner, J. (2004). Telomere length homeostasis is achieved via a switch between telomerase- extendible and -nonextendible states. Cell *117*, 323–335.

Venteicher, A.S., Abreu, E.B., Meng, Z., McCann, K.E., Terns, R.M., Veenstra, T.D., Terns, M.P., and Artandi, S.E. (2009). A human telomerase holoenzyme protein required for Cajal body localization and telomere synthesis. Science *323*, 644–648.

Voss, T.C., and Hager, G.L. (2008). Visualizing chromatin dynamics in intact cells. Biochim. Biophys. Acta *1783*, 2044–2051.

Wellinger, R.J., Wolf, A.J., and Zakian, V.A. (1993). Saccharomyces telomeres acquire single-strand TG1-3 tails late in S phase. Cell *72*, 51–60.

Wellinger, R.J., Ethier, K., Labrecque, P., and Zakian, V.A. (1996). Evidence for a new step in telomere maintenance. Cell *85*, 423–433.

Wotton, D., and Shore, D. (1997). A novel Rap1p-interacting factor, Rif2p, cooperates with Rif1p to regulate telomere length in Saccharomyces cerevisiae. Genes Dev. *11*, 748–760.